

Experimental and theoretical investigation of magnetorheological elastomers

Kostas Danas, Sunny Kankanala, Nicolas Triantafyllidis

► **To cite this version:**

Kostas Danas, Sunny Kankanala, Nicolas Triantafyllidis. Experimental and theoretical investigation of magnetorheological elastomers. 20eme Congres Francais de Mecanique, Aug 2011, Besancon, France. pp.1-5, 2011. <hal-00641538>

HAL Id: hal-00641538

<https://hal-polytechnique.archives-ouvertes.fr/hal-00641538>

Submitted on 16 Nov 2011

HAL is a multi-disciplinary open access archive for the deposit and dissemination of scientific research documents, whether they are published or not. The documents may come from teaching and research institutions in France or abroad, or from public or private research centers.

L'archive ouverte pluridisciplinaire **HAL**, est destinée au dépôt et à la diffusion de documents scientifiques de niveau recherche, publiés ou non, émanant des établissements d'enseignement et de recherche français ou étrangers, des laboratoires publics ou privés.

Experimental and theoretical investigation of magnetorheological elastomers

K. Danas^a, S.V. Kankanala^b, N. Triantafyllidis^a

a. *Laboratoire de Mécanique des Solides, C.N.R.S. UMR7649 & Département de Mécanique, École Polytechnique, ParisTech, 91128 PALAISEAU, France*

b. *BD Medical – Medical Surgical Systems, SANDY UT 84070, USA*

Résumé :

Les élastomères magnétorhéologiques (MREs) font partie des polymères renforcés par des particules ferromagnétiques dont les propriétés mécaniques sont contrôlées par un champ magnétique. En raison du couplage magnétoélastique dans ces matériaux, les MREs sont de plus en plus utilisés pour des applications d'ingénierie. L'objectif de ce travail est (a) l'étude expérimentale des MREs à réponse macroscopique isotrope transverse (les particules forment des chaînes tout le long d'une direction principale) qui sont soumis à un chargement mécanique et magnétique arbitraire et (b) la modélisation macroscopique de ces matériaux en utilisant des fonctions d'énergie isotropes transverses.

Abstract :

Magnetorheological elastomers (MREs) are ferromagnetic particle impregnated elastomers whose mechanical properties are altered by the application of external magnetic fields. Due to their magnetoelastic coupling response, MREs are finding an increasing number of engineering applications. The objective of this work is (a) the experimental study of transversely isotropic MREs (i.e., particles form chains along a certain direction) that are subjected to prestressing and arbitrary magnetic fields and (b) the continuum modeling of these materials using transversely isotropic energy functions.

Mots clefs : 3 maximum : Magnetoelasticity ; Magnetorheological Elastomers ; Magnetomechanical experiments

1 Introduction

Devices made of magneto-rheological elastomers (MREs) have been proposed for a number of engineering applications due to the potentially controllable nature of their mechanical properties [6]. Although there has been a substantial effort in theoretical descriptions of these types of solids (e.g. [3], [5] and [7]), there have not been many studies—to the best knowledge of the authors—dealing with the constitutive modeling and characterization of MREs. Material models for other magnetoelastic solids, however, have been presented in the literature. For example, [9] gave the first characterization of Terfenol-D. In this regard, due to the absence of adequate constitutive description for MREs, it has been difficult to quantify the extent of benefits that a MRE device could offer. The objective of this work is twofold ; first, we present experiments of iron-particle-filled elastomers subjected to prestressing and arbitrary magnetic fields and second, we carry out a phenomenological modeling of these materials.

2 Experiments and modeling

Experiments are carried out for MREs comprising 25% of iron particles of sizes ranging from $0.5\mu\text{m}$ to $5\mu\text{m}$ cured in a 0.8T magnetic field (see upper right micrograph of Fig. 1). The application of a magnetic field during the curing process leads to formation of particle chains aligned with the curing

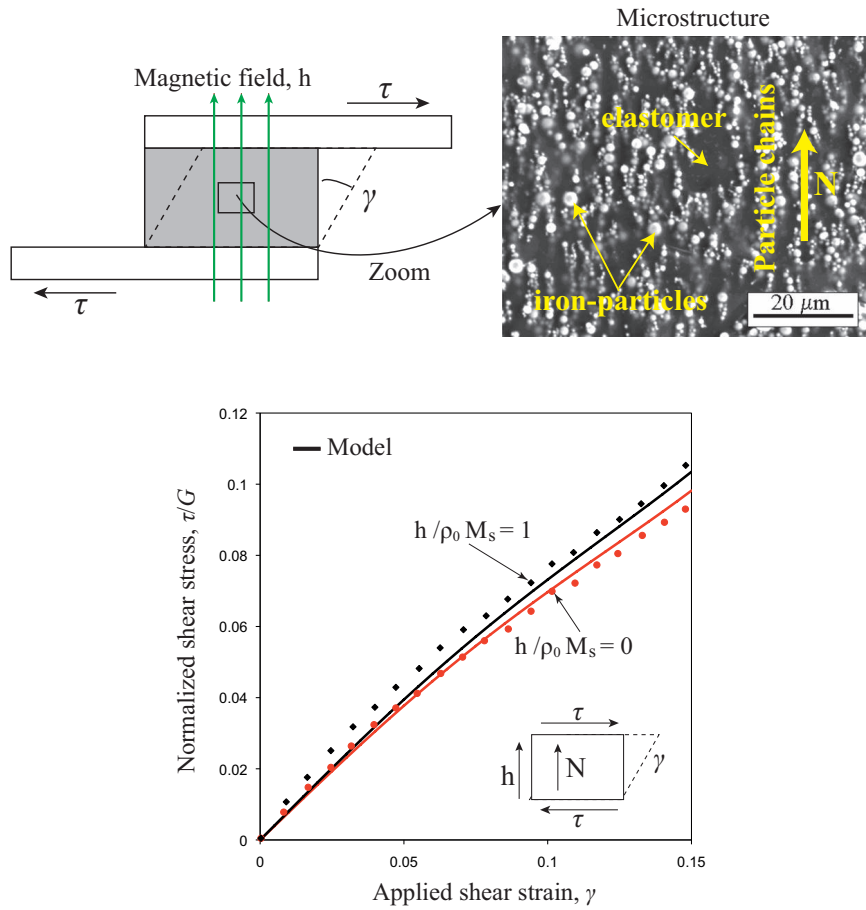


FIGURE 1 – Top left, shows the schematics of a specimen subjected to simple shear in the presence of a magnetic field. Top right shows an electron micrograph (from [6]) of a MRE comprising 25% of iron particles of sizes ranging from $0.5\mu\text{m}$ to $5\mu\text{m}$ cured in a magnetic field. The application of a magnetic field during the curing process leads to formation of particle chains aligned with the curing field direction. In the bottom figure are experimental (discrete marks) and theoretical (solid lines) results showing the influence of the magnetic field on the MRE's simple shear response with G denoting the shear modulus.

field direction. The experiments involve three different setups; (a) simple shear tests where the particle chains are initially aligned with the applied magnetic field, as shown in Fig. 1, (b) uniaxial stress tests in the direction of a magnetic field which is aligned with the particle chains, as shown in Fig. 2a, and (c) uniaxial stress tests in the direction of a magnetic field which is perpendicular to the particle chains, as shown in Fig. 2b.

The experimentally observed response of the MRE (discrete symbols for experiments) when subjected to simple shear loading in the absence or in the presence of a magnetic field parallel to the particle chain orientation is shown in Fig.1. Notice that the initial longitudinal shear modulus G appears to be rather insensitive to the presence of a strong magnetic field, while the material becomes stiffer under the presence of a magnetic field once shear strain increases.

In turn, the magnetostriction strain $\Delta\epsilon$ versus the applied nondimensional magnetic field $h/\rho_0 M_s$ is shown in Fig. 2 for uniaxial stress tests. In Fig. 2a, the magnetostriction is plotted for different preloads σ/G , which are aligned with the applied magnetic field and the particle chain ($\mathbf{h} \parallel \mathbf{N}$). In general, the magnitude of magnetostriction increases with the magnitude of the nondimensional preloads. Elongation strains increase from 0.34% for $\sigma/G = 0$ to about 0.48% for $\sigma/G = -0.288$. By comparison, the strains in the MREs are about double those seen in a magnetostrictive material like Terfenol-D (0.15% to 0.2%, [9]). Negative strains are seen for all tensile prestresses with saturation strains of about 0.6% for $\sigma/G = +0.288$. Although a small amount of hysteresis is present in these experiments, especially near saturation levels, it is ignored in the subsequent modeling. Interestingly,

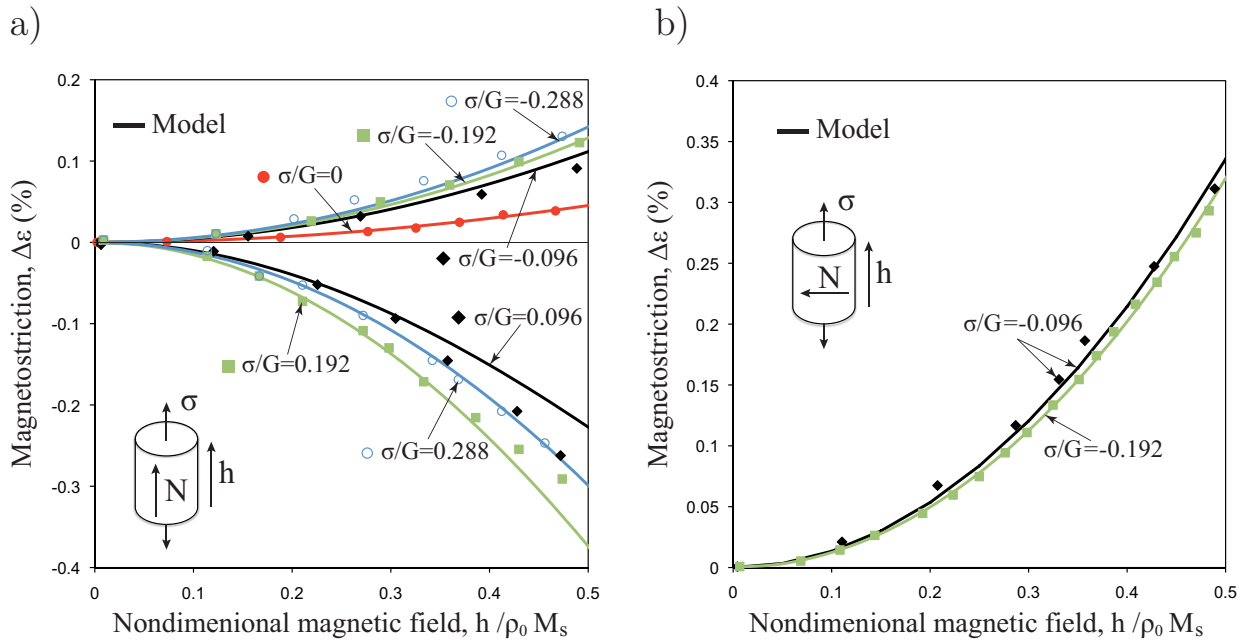


FIGURE 2 – Comparison for small magnetic fields between experimental (discrete symbols) and modeling (continuous lines) results for the magnetostriction $\Delta\varepsilon$ versus the applied nondimensional magnetic field $h/\rho_0 M_s$ for various prestresses, σ/G , aligned with the applied magnetic field. Part (a) and (b) correspond to the cases where the particle chains are parallel ($\mathbf{h} \parallel \mathbf{N}$) and perpendicular ($\mathbf{h} \perp \mathbf{N}$), respectively, to the applied magnetic field.

the magnetostriction response is not symmetric with respect to the sign of the prestress in Fig. 2a. Notice that the sample expands ($\Delta\varepsilon > 0$) for zero or negative prestresses ($-0.288 \leq \sigma/G \leq 0$) and contracts ($\Delta\varepsilon < 0$) for adequately large tensile prestresses ($0.096 \leq \sigma/G \leq 0.288$). This implies a strong nonlinear effect of the applied prestress on the resulting magnetostriction. In turn, in Fig. 2b, we investigate the influence of particle chain orientation with respect to the applied magnetic field for two different compressive preloads. Notice that the initial curvature of the $\Delta\varepsilon - h$ response increases significantly for the case of particle chain orientation perpendicular to the applied magnetic field ($\mathbf{h} \perp \mathbf{N}$), as also do the corresponding saturation strains which are three to four times larger (depending on prestress) than those corresponding to the parallel case ($\mathbf{h} \parallel \mathbf{N}$).

The second part of this work pertains in finding an energy density function $\hat{\psi}$ that best fits the experiments reported above. As already pointed out, the material under investigation is a transversely isotropic composite since the iron particles form chains along a certain direction. This implies that the free energy density $\hat{\psi}$ should also depend on the unit vector \mathbf{N} (see Fig. 1), which defines the initial orientation of the particle chains. Thus,

$$\hat{\psi} = \hat{\psi}(\mathbf{C}, \mathbf{N}, \mathbf{M}), \quad \mathbf{C} = \mathbf{F}^T \bullet \mathbf{F}, \quad \mathbf{N} \bullet \mathbf{N} = 1, \quad (1)$$

where \mathbf{F} is the material's deformation gradient (\mathbf{F}^T denotes its transpose), \mathbf{C} denotes the right "Cauchy-Green" tensor and \mathbf{M} the specific magnetization.

Using the general theory of transversely isotropic functions [1, 2] that depend on a rank-two tensor, the right Cauchy-Green tensor \mathbf{C} , and two vectors, the orientation vector \mathbf{N} and the magnetization \mathbf{M} , one obtains that $\hat{\psi}$ is a function of ten independent invariants, namely

$$\begin{aligned} I_1 &= \text{tr} \mathbf{C}, & I_2 &= \frac{1}{2} [(\text{tr} \mathbf{C})^2 - \text{tr} \mathbf{C}^2], & I_3 &= \det \mathbf{C}, \\ I_4 &= \mathbf{N} \bullet \mathbf{C} \bullet \mathbf{N}, & I_5 &= \mathbf{N} \bullet \mathbf{C}^2 \bullet \mathbf{N}, \\ I_6 &= \mathbf{M} \bullet \mathbf{M}, & I_7 &= \mathbf{M} \bullet \mathbf{C} \bullet \mathbf{M}, & I_8 &= \mathbf{M} \bullet \mathbf{C}^2 \bullet \mathbf{M}, \\ I_9 &= (\mathbf{M} \bullet \mathbf{N})^2, & I_{10} &= (\mathbf{M} \bullet \mathbf{N})(\mathbf{M} \bullet \mathbf{C} \bullet \mathbf{N}). \end{aligned} \quad (2)$$

Following [7] (*c.f.* relations (2.42) and (2.44) in that reference), we obtain the following expressions for the total Cauchy stress $\boldsymbol{\sigma}$ and the magnetic field \mathbf{h}

$$\boldsymbol{\sigma} = \rho \left[2\mathbf{F} \bullet \frac{\partial \hat{\psi}}{\partial \mathbf{C}} \bullet \mathbf{F}^T + \mu_0 (\mathbf{M}\mathbf{h} + \mathbf{h}\mathbf{M}) \right] + \mu_0 \left[\mathbf{h}\mathbf{h} - \frac{1}{2}(\mathbf{h} \bullet \mathbf{h})\mathbf{I} \right], \quad \mu_0 \mathbf{h} = \frac{\partial \hat{\psi}}{\partial \mathbf{M}}, \quad (3)$$

where ρ is the current material density. Note that in vacuum ($\rho = 0$), the total stress is non-zero and equals the Maxwell stress $\mu_0[\mathbf{h}\mathbf{h} - (1/2)(\mathbf{h} \bullet \mathbf{h})\mathbf{I}]$.

Making use of the above definitions, the incompressibility of the MRE (i.e., $I_3 = 1$ and consequently $\rho = \rho_0$ with ρ_0 denoting the initial density) and cumbersome algebra (not shown here due to restrictions in space but will be presented elsewhere), we propose the following simple expression for the energy density

$$\hat{\psi} = \frac{\rho_0 G}{2} \left\{ C_1 \sum_{k=1}^5 d_{1k} (I_1 - 3)^k + C_4 \sum_{k=2}^4 d_{4k} (I_4 - 1)^k + C_6 \frac{I_6}{M_s^2} + C_7 \frac{I_7}{M_s^2} + C_8 \frac{I_8}{M_s^2} + C_9 \frac{I_9}{M_s^2} + C_{10} \frac{I_{10}}{M_s^2} \right\}, \quad (4)$$

$$(5)$$

where the coefficients are given by

$$\begin{aligned} C_1 &= 1, & d_{11} &= 1, & d_{12} &= -7, & d_{13} &= 120, & d_{14} &= -700, & d_{15} &= 3000, \\ C_4 &= 0.103, & d_{42} &= 1, & d_{43} &= -21, & d_{44} &= 90, & & & & \\ C_6 &= 0.36, & C_7 &= -0.32, & C_8 &= 0.108, & C_9 &= -0.12, & C_{10} &= 0.075. & & \end{aligned} \quad (6)$$

Notice in (6) that two of the coefficients, C_7 and C_9 are negative. Nevertheless, the overall energy density $\hat{\psi}$ remains always positive, since $C_6 > C_9$ (with $I_9 = I_6$ for $\mathbf{h} \parallel \mathbf{N}$ and $I_9 = 0$ for $\mathbf{h} \perp \mathbf{N}$) and $C_6 + C_7 \mathbf{C} + C_8 \mathbf{C}^2 > 0$ for all \mathbf{C} .

Theoretical predictions, based on the energy density of equation (5) are compared to experimental results in the case of simple shear loading as shown in the bottom of Fig. 1 and a uniaxial stress test in the direction of a magnetic field which is (a) aligned with the particle chains (see Fig. 2a) and (b) perpendicular to the particle chains (see Fig. 2b). In all three cases, the model predicts well the experimental response of the MRE.

It should be pointed out here that the magnetic field effect on the material's simple shear response is much less pronounced (of the order of 10% for $\gamma = 0.15$) than in the case of magnetostriction under uniaxial stress states (not shown here due to restrictions in space but will be presented elsewhere). This indicates that if maximum magnetoelastic coupling effects are required in application, shearing is the least effective method to achieve them.

3 Conclusions

The present experimental/theoretical investigation for MREs subjected to coupled mechanical and magnetic loading gives a good agreement with experiments up to relatively moderate magnetic fields and is satisfactorily extended to include magnetic fields near saturation. The work shows the adequacy of the anisotropic, finite strain continuum formulation for the description of these materials. The study also demonstrates the importance of microgeometry in the macroscopic magnetoelastic coupling response of the composite. Given the need in applications to produce MREs with strong magnetoelastic coupling, it is desirable to build a) microscopic models to study these coupling mechanisms in detail and b) mean-field (i.e., homogenization) models to investigate more efficiently the influence of matrix properties, particle distribution and shape on the macroscopic magnetomechanical response of these composites. On the practical side, mean field theories are a valuable tool to optimize coupling properties (e.g., [8], [4]) in these materials. Studies in these directions are currently under way by the authors.

Références

- [1] Adkins, J., 1959. Symmetry relations for orthotropic and transversely isotropic materials. *Arch. Rat. Mech. Anal.* 4, p. 193–213.
- [2] Adkins, J., 1960. Further symmetry relations for transversely isotropic materials. *Arch. Rat. Mech. Anal.*, 5, p. 263–274.
- [3] Borcea, L., Bruno, O., 2001, On the magneto-elastic properties of elastomer-ferromagnet composites, *J. Mech. Phys. Solids* 49, 2877 – 2919.
- [4] Corcolle, R., Daniel, L., Bouillault, F., 2009, Intraphase fluctuations in heterogeneous magnetic materials. *J. Appl. Phys.* **105**, pp. 123913.
- [5] Dorfmann, A., Ogden, R.W., 2003, Magnetoelastic modelling of elastomers, *Eur. J. Mech. A/Solids* 22, 497 – 507.
- [6] Ginder, J., Nichols, M., Elie, L., Tardiff, J., 1999 Magnetorheological elastomers : Magnetorheological elastomers : properties and applications, *Smart Structures and Materials 1999 : Smart Materials Technologies Ed. by M. Wuttig, Proc. of SPIE*,3675, 131–138.
- [7] Kankanala, S.V., Triantafyllidis, N., 2004, On finitely strained magnetorheological elastomers, *J. Mech. Phys. Solids* 52, 2869 – 2908.
- [8] Kuo, H.Y., Slinger, A., Bhattacharya, K., 2010. Optimization of magnetoelectricity in piezoelectric–magnetostrictive bilayers. *Smart Materials and Structures*19, pp. 125010.
- [9] Moffett, M.B., Clark, A.E., Wun-Fogle, M., Linberg, J., Teter, J. P., McLaughlin, E.A., 1991, Characterization of Terfenol-D for magnetostrictive transducers, *J. Acoust. Soc. America* 89, 1448 – 1455.